Journal of Power Sources 191 (2009) 344–350

Contents lists available at ScienceDirect

Journal of Power Sources

journal homepage: www.elsevier.com/locate/jpowsour

Stability of Pt–Ni/C (1:1) and Pt/C electrocatalysts as cathode materials for polymer electrolyte fuel cells: Effect of ageing tests

Sabrina C. Zignani [a], Ermete Antolini [a,b], Ernesto R. Gonzalez [a,*]

[a] Instituto de Química de São Carlos, USP, C.P. 780, São Carlos 13560-970, SP, Brazil
[b] Scuola di Scienza dei Materiali, Via 25 aprile 22, 16016 Cogoleto, Genova, Italy

ARTICLE INFO

Article history:
Received 10 December 2008
Received in revised form 16 January 2009
Accepted 28 January 2009
Available online 7 February 2009

Keywords:
Oxygen reduction
Pt–Ni/C electrocatalysts
PEM fuel cell
Dissolution
Stability

ABSTRACT

Carbon supported Pt and Pt–Ni (1:1) nanoparticles were prepared by reduction of metal precursors with $NaBH_4$. XRD analysis indicated that only a small amount of Ni alloyed with Pt (Ni atomic fraction in the alloy about 0.05). The as-prepared catalysts were submitted to chronoamperometry (CA) measurements to evaluate their activity for the oxygen reduction reaction (ORR). CA measurements showed that the ORR activity of the as-prepared Ni-containing catalyst was higher than that of pure Pt. Then, their stability was studied by submitting these catalysts to durability tests involving either 30 h of constant potential (CP, 0.8 V vs. RHE) operation or repetitive potential cycling (RPC, 1000 cycles) between 0.5 and 1.0 V vs. RHE at 20 mV s^{-1}. After 30 h of CP operation at 0.8 V vs. RHE, loss of all non-alloyed Ni, partial dissolution of the Pt–Ni alloy and an increase of the crystallite size was observed for the Pt–Ni/C catalyst. The ORR activity of the Pt–Ni/C catalyst was almost stable, whereas the ORR activity of Pt/C slightly decreased with respect to the as-prepared catalyst. Loss of all non-alloyed and part of alloyed Ni was observed for the Pt–Ni/C catalyst following repetitive potential cycling. Conversely to the results of 30 h of CP operation at 0.8 V vs. RHE, after RPC the ORR activity of Pt–Ni/C was lower than that of both as-prepared Pt–Ni/C and cycled Pt/C. This result was explained in terms of Pt surface enrichment and crystallite size increase for the Pt–Ni/C catalyst.

1. Introduction

Platinum catalysts still serve as state of the art electrocatalysts in low temperature polymer electrolyte fuel cells (PEMFCs) [1]. However, due to kinetic limitations of the oxygen reduction reaction (ORR) the cathodic overpotential losses amount to 0.3–0.4 V under typical PEMFC operating conditions [1]. The reduction of the cathodic cell voltage losses requires the development of an ORR catalyst more active than platinum. The alloys of transition metals, such as V, Cr, Co, Ti and Ni, with platinum have been found to exhibit significantly higher electrocatalytic activities towards the oxygen reduction reaction than platinum alone in low temperature fuel cells [2–11]. The improvement in the ORR electrocatalysis of Pt-alloys has been ascribed to different structural changes caused by alloying. Jalan and Taylor [2] claimed that the increased Pt catalytic activity observed for Pt-alloys is related to the shortening of the Pt–Pt interatomic distance. Paffett et al. [4] ascribed the enhancement of ORR activity on the alloys to surface roughening, caused by the dissolution of the more oxidisable alloying component. Min et al. [9] and Mukerjee et al. [12] attributed the improvement of Pt catalytic activity to combined electronic (Pt d-band vacancy) and geometric (Pt–Pt bond distance) effects. Recently, Stamenkovic et al. [13,14] attributed the enhancement of the catalytic activity for ORR on Pt_3Ni and Pt_3Co surface alloys to the inhibition of $Pt–OH_{ad}$ formation on Pt sites surrounded by "oxide"-covered Ni and Co atoms.

Various studies focused on the ORR activity of both bulk and carbon supported Pt–Ni catalysts. Drillet et al. [15] studied the electrochemical oxygen reduction reaction at Pt and Pt alloyed with 30 at.% Ni in 1 M H_2SO_4 by means of rotating disc electrode. Unsupported $Pt_{70}Ni_{30}$ catalyst was prepared by melting together Pt and Ni pellets in a vacuum arc. They found that in pure sulphuric acid, the overpotential of ORR at 1 mA cm^{-2} is about 80 mV lower at $Pt_{70}Ni_{30}$ than at pure Pt. Toda et al. [8] studied the ORR activity in perchloric acid solution of bulk Pt alloys with Ni, Co and Fe at room temperature. Maximum activity was observed at ca. 30%, 40% and 50% content of Ni, Co and Fe, respectively, by which 10, 15 and 20 times larger kinetic current densities than that of pure Pt were attained. By X-ray photoelectron spectroscopy (XPS) measurements they found that Ni, Co or Fe disappeared from all the alloy surface layers and the active surfaces were covered by a Pt skin of a few monolayers. The authors ascribed the high ORR activity of these catalysts to the modification of the electronic structure of the Pt skin layer originating from that of the bulk alloys. More recently,

* Corresponding author. Tel.: +55 16 33739899; fax: +55 16 33739952.
E-mail address: ernesto@iqsc.usp.br (E.R. Gonzalez).

0378-7753/$ – see front matter © 2009 Elsevier B.V. All rights reserved.
doi:10.1016/j.jpowsour.2009.01.088

the temperature dependence of ORR activity on the same bulk alloy catalysts in 0.1 M $HClO_4$ solution from 20 to 90 °C was investigated by the same research group [16]. They found that in the temperature range of 20–50 °C the apparent rate constants k_{app} for ORR at Pt–M electrodes were 2.4–4 times larger than that on a pure Pt electrode. The k_{app} values at the alloy electrodes decreased when elevating the temperature above 60 °C, and settled to almost the same values as on the Pt electrode. Mukerjee et al. [6,12] studied the electrocatalysis of oxygen reduction on carbon supported Pt–Ni and other Pt-based binary alloys in the atomic ratio Pt:M = 3:1 in polymer electrolyte fuel cells. They found a two- to threefold enhancement of the ORR activity on these alloy catalysts compared to pure Pt. Paulus et al. [10] investigated the ORR activity of commercial Pt–Ni/C catalysts in the Pt:Ni atomic ratio 75:25 and 50:50. Kinetic analysis in comparison to pure Pt revealed a small activity enhancement (per Pt surface atom) of ca. 1.5 for the 25 at.% Ni catalyst. The 50 at.% Ni catalyst, instead, was less active than the Pt standard and unstable at oxygen electrode potentials. Yang et al. [17] investigated the effect of the composition on ORR activity of Pt–Ni alloy catalysts prepared by a Pt-carbonyl route. The maximum activity of the Pt-based catalysts was found with ca. 30–40 at.% Ni content in the alloys, corresponding to a Pt–Pt mean interatomic distance from ca. 0.2704 to 0.2724 nm. Thus, the authors concluded that the high activity of these catalysts for the ORR comes from the favorable Pt–Pt mean interatomic distance caused by nickel alloying and the disordered surface structures induced by the particle size.

Electrode durability is an important factor limiting the commercialization of PEMFCs. Metal particle sintering, metal dissolution and carbon support corrosion all contribute to cathode catalyst degradation. The results of the different tests on the stability of Pt–M alloy catalysts in fuel cell conditions and the consequences on the electrocatalytic activity and cell performance have been reviewed by Antolini et al. [18]. It has to be underlined, however, that the operating environment of the polymer electrolyte fuel cells is not nearly as severe as that of the PAFCs, then a better stability of these alloy catalysts in the PEFC environment would be expected. As a consequence, evaluating durability in PEM fuel cells requires longer testing times. Colon-Mercado et al. [19] developed an accelerated durability test to evaluate the long-term performance of Pt_3Ni catalysts. They found that a strong correlation exists between the amount of Ni dissolved and the oxygen reduction activity of the catalyst.

In this laboratory, Pt–Co and Pt–Ni catalysts have been studied and found more active than Pt for the ORR. Also, they were found more tolerant to methanol in DMFCs. However, there was some concern about the stability and durability of those materials and the effects of degradation on activity, so a first study of these aspects was carried out recently with Pt–Co materials [20]. Following this line of research, in the present work we have prepared carbon supported Pt and Pt–Ni (Pt:Ni nominal atomic ratio 1:1) catalysts by reduction of Pt and Ni precursors with $NaBH_4$ at room temperature, to avoid the sintering of metal particles that takes place when the synthesis of the catalyst is carried out at high temperatures [21]. Then, accelerated durability tests, as 30 h of constant potential (CP) operation at 0.8 V vs. RHE and repetitive potential cycling (RPC) in the range 0.5–1.0 V vs. RHE were carried out on these catalysts to evaluate their long-term performance.

2. Experimental

Carbon supported Pt and Pt–Ni (nominal Pt:Ni atomic ratio 1:1) electrocatalysts were prepared by a low temperature method, using sodium borohydride as the reducing agent. High surface area carbon (Vulcan XC-72R, Cabot, 240 $m^2\ g^{-1}$) was impregnated with a solution of chloroplatinic acid ($H_2PtCl_6{\cdot}6H_2O$, Johnson Matthey) and, in the case of Pt–Ni, nickel hydroxide ($Ni(OH)_2{\cdot}6H_2O$, Aldrich) solution. The metals were then reduced at room temperature with a sodium borohydride solution, which was slowly added to the precursor solution under sonication. The material was 20 wt.% metal on carbon.

The atomic ratio of the Pt–Ni/C catalysts was determined by the EDX technique coupled to a scanning electron microscope LEO Mod. 440 with a silicon detector with Be window and applying 20 keV.

X-ray diffractograms of the electrocatalysts were obtained in a universal diffractometer Carl Zeiss-Jena, URD-6, operating with Cu $K\alpha$ radiation (λ = 0.15406 nm) generated at 40 kV and 20 mA. Scans were done at 3 min^{-1} for 2θ values between 20 and 100°. It has to be remarked that the XRD measurements on as-prepared and thermally treated catalysts were carried out on the catalyst powder, whereas the XRD analysis on the catalysts submitted to RPC were carried out on the electrode. The lattice parameters were obtained from the Pt (3 1 1) peaks. The crystallite sizes were obtained from the Pt (2 2 0) reflexion.

In situ X-ray absorption spectroscopy (XAS) measurements were performed in the Pt L_{III} absorption edges, using a spectro-electrochemical cell [22]. The working electrodes consisted of pellets formed with the dispersed catalysts agglutinated with PTFE (ca. 40 wt.%) and containing 6 mg cm^{-2}. The counter electrode was a Pt screen. This electrode was cut in the center, in order to allow the free passage of the X-ray beam. Prior to the experiments, the working electrodes were soaked in the electrolyte for at least 48 h. XAS experiments were carried out at 0.8 V vs. RHE, after conditioning the electrodes by cycling between 0.5 and 1.0 V vs. RHE. Results presented here correspond to the average of at least two independent measurements.

All the XAS experiments were conducted at the D04B-XAS1 beam line in the Brazilian Synchrotron Light Laboratory (LNLS), Brazil. The data acquisition system for XAS comprised three ionization detectors (incidence I_0, transmision I_t and reference I_r). The reference channel was employed primarily for internal calibration of the edge positions by using a foil of the pure metal. Nitrogen was used in the I_0, I_t and I_r chambers. Owing to the low critical energy of the LNLS storage ring (2.08 keV), third-order harmonic contamination of the Si (1 1 1) monochromatic beam is expected to be negligible above 5 eV [23].

The computer program used for the analysis of the XAS data was the WinXAS package [24]. The data analysis was done according to procedures described in detail in the literature [25,26]. Briefly, the X-ray absorption near-edge structure (XANES) spectra were first corrected for the background absorption by fitting the pre-edge data (from −60 to −20 eV below the edge) to a linear formula from the data over the energy range of interest. Next, the spectra were calibrated for the edge position using the second derivative of the inflection point at the edge jump of the data from the reference channel.

In order to test the electrochemical behaviour in sulphuric acid, the electrocatalysts were used to make two layer gas diffusion electrodes (GDEs). A diffusion layer was made with carbon powder (Vulcan XC-72R) and 30 wt.% polytetrafluoroethylene (PTFE) and applied over a carbon cloth (PWB-3, Stackpole). On top of this layer, the electrocatalyst was applied in the form of a homogeneous dispersion of Pt–Ni/C, or Pt/C, Nafion® solution (5 wt.%, Aldrich) and isopropanol (Merck). All electrodes were made to contain 0.4 mg cm^{-2} of metal.

Cyclic voltammograms and linear sweep voltammograms (LSV) were recorded in a single cell in 0.5 M H_2SO_4 solution. Argon (White Martins) was passed for 30 min to eliminate oxygen. Gas diffusion electrodes containing Pt/C and Pt–Ni/C electrocatalysts were used as working electrodes. A hydrogen electrode was used as reference and a platinum foil electrode as auxiliary. The CVs were recorded in the range 0.5–1.0 V vs. a reversible hydrogen electrode (RHE) at a

scan rate of 20 mV s^{-1}. The number of cycles was 1000. The electrochemical half cell was built in PTFE with a volume of approximately 70 mL. After the voltammetric study, oxygen was passed for 30 min to saturate the solution.

Chronoamperometry (CA) experiments were performed at room temperature at 0.8 V for 3600 s. The experiments were done at room temperature with a 1285 A Solartron Potentiostat connected to a personal computer and using the software CorrWare for Windows (Scribner). Regarding the durability tests of 30 h of constant potential operation at 0.8 V, changes in the composition of the H_2SO_4 solution, indicative of metal dissolution, were observed after 5 h of testing.

Two types of constant potential (CP) experiments were carried out at 0.8 V also in a 0.5 M H_2SO_4 solution. Normal chronoamperometry (CA) was performed for 3600 s to test the activity of the catalysts under quasi-steady state conditions. Extended experiments for 30 h were performed separately to evaluate the durability of the catalysts. In this case, every 5 h of testing the H_2SO_4 solution in the cell was changed by a fresh one and submitted to atomic absorption analysis to determine Pt and Ni eventually dissolved. Atomic adsorption (AA) determinations were carried out using an Atomic Adsorption Spectrophotometer HITACHI Z-8100.

The sequence of experiments in this work was as follows. The as-prepared catalysts were submitted to CA experiments in an oxygen-saturated solution to evaluate the activity for the ORR. Next, under an inert argon atmosphere, they were submitted to durability tests involving either 30 h of constant potential (0.8 V vs. RHE) operation or repetitive potential cycling (1000 cycles) between 0.5 and 1.0 V vs. RHE at 20 mV s^{-1}. After the durability test, the solution was again saturated with oxygen and CA experiments were performed again.

3. Results and discussion

3.1. Characterization of the materials

The EDX compositions of the carbon supported electrocatalysts, as-prepared and following the stability tests, are reported in Table 1. The value of Pt:Ni atomic ratio of the as-prepared catalyst was 45:55, near to the nominal composition. After both stability tests Ni content in the catalyst considerably decreased.

Fig. 1 shows the XRD pattern of as-prepared carbon supported Pt and Pt–Ni electrocatalysts, and of Pt–Ni/C following the stability tests. All the XRD patterns show the five main reflexions corresponding to the planes (1 1 1), (2 0 0), (2 2 0), (3 1 1) and (2 2 2), characteristic of the face-centered cubic (fcc) structure of Pt. In the binary Pt–Ni electrocatalysts these five diffraction peaks were shifted to higher values of 2θ, which is indicative of a contraction of the lattice, due to the alloy formation between Pt and Ni. No characteristic peaks of metallic Ni or Ni oxides were detected, but their presence cannot be discarded because they may be present in a small amount or even in an amorphous form. The lattice parameters of all the catalysts are given in Table 1. It is known that in the composition range from 0 to 50 at.% Pt and Ni form a substitutional continuous solid solution and two ordered phases [27]. The dependence of the lattice parameter of unsupported Pt–Ni alloys on Ni

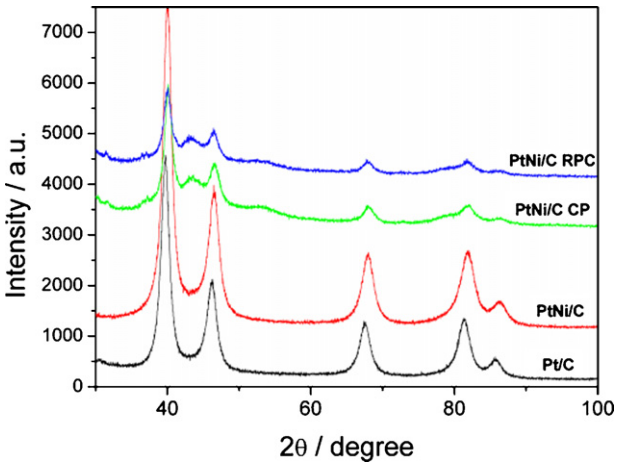

Fig. 1. XRD diffractograms of as-prepared Pt/C and Pt–Ni/C, and tested Pt–Ni/C electrocatalysts.

contents follows Vegard's law and is reported in Ref. [28]. On this basis, the Ni atomic fraction in the Pt–Ni alloy (x) was evaluated by the relationship:

$$x = \left[\frac{(a - a_o)}{(a_s - a_o)}\right] x_s \quad (1)$$

where a_o and a_s are the lattice parameters of Pt (0.3919 nm) and Pt_3Ni (0.382 nm [28]), and x_s is the Ni atomic fraction (0.25) in the Pt_3Ni catalyst. The amount of alloyed Ni was estimated to be about 5.2 at.% for the as-prepared Pt–Ni/C catalyst, i.e. a poor degree of alloying was obtained. From these results, it can be inferred that in the as-prepared Pt–Ni/C electrocatalyst most of the nickel is in a non-alloyed form (as Ni metal or NiO_x species). Regarding the Pt–Ni catalysts prepared by reduction of Pt and Ni precursors with $NaBH_4$ at room temperature, it seems that the amount of Ni alloyed is independent of the Ni content in the catalyst, as shown in Fig. 2, where the lattice parameter of Pt–Ni catalysts (this work and Refs. [29,30]), all prepared by reduction of Pt and Ni precursors with $NaBH_4$ at room temperature, is plotted against the EDX composition.Following both stability tests, the Ni content in the alloy was almost the same than that in the as-prepared catalyst, indicating the absence of Ni de-alloying during durability tests. In particular, after 30 h of constant potential operation at 0.8 V, the XRD composition was the same than the EDX composition. The amount of Ni and Pt lost to the solution during the durability test at constant potential was obtained from atomic absorption analysis, and led to the conclusion that the most part of Ni loss (>85%), coming overall from non-alloyed Ni, occurs in the first 7 h of the operation test, as shown in Fig. 3, where the amount of Ni and Pt loss, relative to the total metal loss, is plotted against CP operation time. Above 7 h of CP, Pt and Ni loss almost linearly increased with operation time: this result indicates that metal loss comes from the dissolution of the Pt–Ni alloy. Following repetitive potential cycling, instead, the Pt/Ni atomic ratio by XRD was higher than Pt/Ni by EDX. This could reveal the loss of all non-alloyed Ni, and dissolution of part of the

Table 1
EDX composition, lattice parameter, Ni atomic fraction in the alloy from Eq. (1) (x_{Ni}) and crystallite size of Pt/C and Pt–Ni/C catalysts, as-prepared and after durability tests.

Catalyst	EDX composition (Pt:Ni/at. %)	Lattice parameter from (3 1 1) peak (nm)	x_{Ni} (%)	Crystallite size from (2 2 0) peak (nm)
Pt/C	–	0.39190 (24)		5.6
Pt–Ni/C as-prepared	45:55	0.38988 (20)	5.2 ± 0.5	5.1
Pt–Ni/C after 30 h CP	95:05	0.38976 (18)	5.6 ± 0.5	6.3
Pt–Ni/C after RPC	98:02	0.39008 (25)	4.7 ± 0.6	5.9
Pt/C after RPC[a]		0.39224		6.6

[a] Data for Pt/C after RPC from Ref. [20].

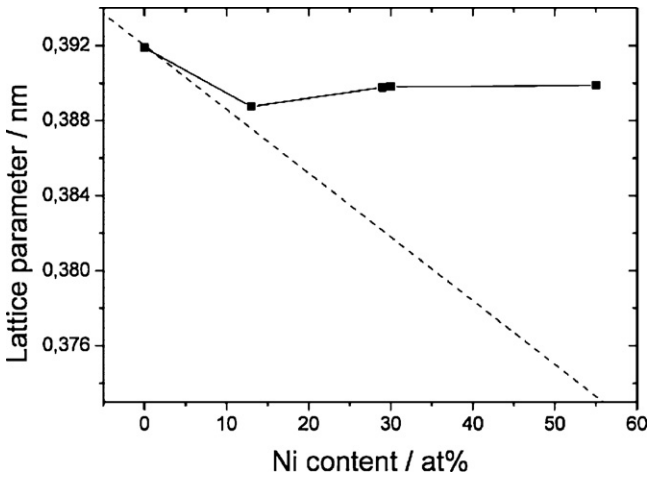

Fig. 2. Pt–Ni lattice parameter vs. EDX composition. The values of the lattice parameter for the EDX compositions of 13% and 29% were reported in Ref. [28], and for the EDX composition of 30% in Ref. [29]. Dashed line: lattice parameter vs. Ni content in the alloy according to Vegard's law, from Ref. [26].

Pt–Ni alloy, with reprecipitation of Pt (but not of Ni) on the catalyst surface, as observed in the case of cycled Pt–Co/C [20].

The crystallite size of as-prepared Pt–Ni/C and Pt/C, and tested Pt–Ni/C, calculated from XRD measurements, is reported in Table 1. The crystallite size of as-prepared Pt–Ni/C was slightly lower than that of Pt/C. After durability tests an increase of 15–20% of crystallite size was observed.

Fig. 4a shows the XANES spectra at the Pt L_3 edge at 0.8 V for the as-prepared Pt–Ni/C and Pt/C electrocatalysts, and for the reference Pt foil. A significantly higher intensity of the Pt L_3 white line of Pt/C compared to Pt–Ni/C and the reference Pt foil was observed. Normally, the intensity of the Pt L_3 edge increases with the increase in Pt d-band vacancy, in this case due to the adsorption of oxygenated species [31]. The affinity of OH chemisorption on Pt depends on both the metal particle size and alloying. It is known that there is an increase in the affinity of OH chemisorption on Pt as the metal particle size decreases [32] and the amount of M in Pt–M also decreases in Pt alloys [31]. It has to be remarked that the ORR activity decreases with an increase of adsorption of OH on the Pt active sites [33]. The higher value of the Pt d-band vacancy for the Pt/C catalyst can be explained on the basis of the chemisorption of oxygenated species from the electrolyte solution on the Pt surface at 0.8 V vs. RHE. In the alloy catalysts such an increase in the Pt d-band vacancy is lower than in Pt. This could be accounted for by the lower affinity of OH chemisorption on Pt in the Pt alloys, unlike that on the Pt/C electrocatalysts [31]. Thus, being the Pt–Ni particle size slightly smaller than the Pt particle size, XANES results attest the formation of a Pt–Ni alloy, in agreement with the XRD results. Fig. 4b shows the XANES spectra at the Pt L_3 edge at 0.8 V for the Pt–Ni/C and Pt/C electrocatalysts after repetitive potential cycling. A decrease of the white line intensity was observed for Pt/C with respect to the as-prepared catalyst, due to the increase of particle size. On the contrary, the white line intensity for Pt–Ni/C was almost the same as that of the as-prepared catalyst. This result could be ascribed to the counteracting effect on Pt d-band vacancy of particle growth and Pt re-deposition on the catalyst surface (see below). The Pt L_3 white lines of Pt–Ni/C and Pt/C after repetitive potential cycling presented no substantial difference.

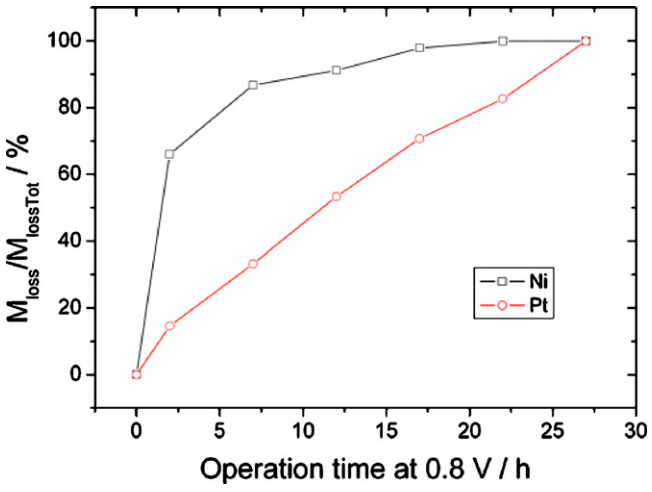

Fig. 3. Dependence of Pt and Ni loss on the operation time at constant potential.

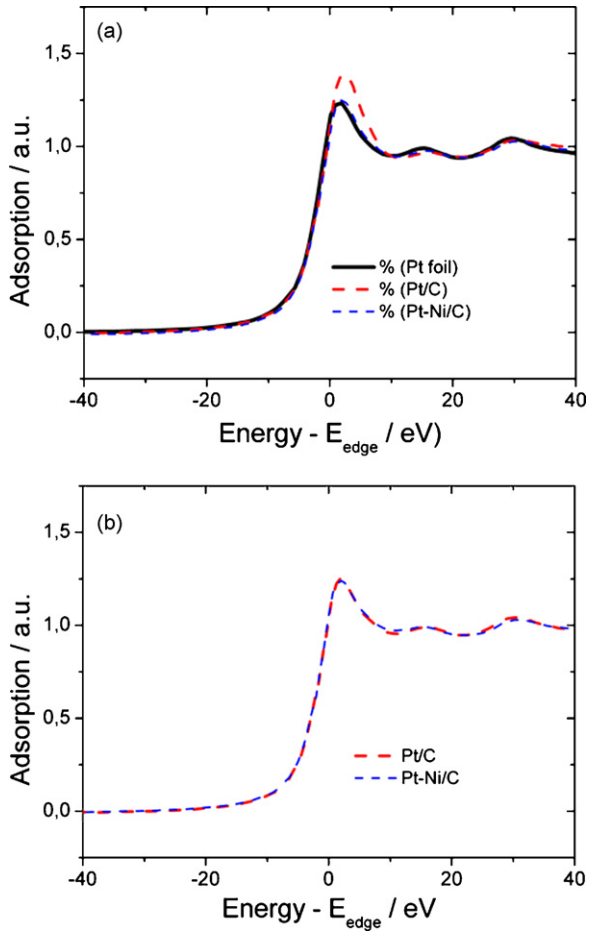

Fig. 4. Pt L_3 XANES spectra at 0.8 V for carbon supported Pt and Pt–Ni alloy electrocatalysts relative to a Pt reference foil in 0.5 mol L^{-1} H_2SO_4. (a) As-prepared catalysts and (b) catalysts after repetitive potential cycling.

3.2. Electrochemical experiments

3.2.1. As-prepared catalysts

The electrochemical activity for oxygen reduction of as-prepared Pt/C and Pt–Ni/C catalysts was investigated by chronoamperometry (CA) tests at 0.8 V vs. RHE for 3600 s at room temperature, and the results are shown in Fig. 5. It can be clearly seen that the currents for oxygen reduction on both the catalysts dropped rapidly at first and then became relatively stable. The initial surge of the current is possibly due to the charging current. As can be seen in Fig. 5, the steady state current density on the as-prepared Pt–Ni/C catalyst was significantly higher than that on Pt/C.

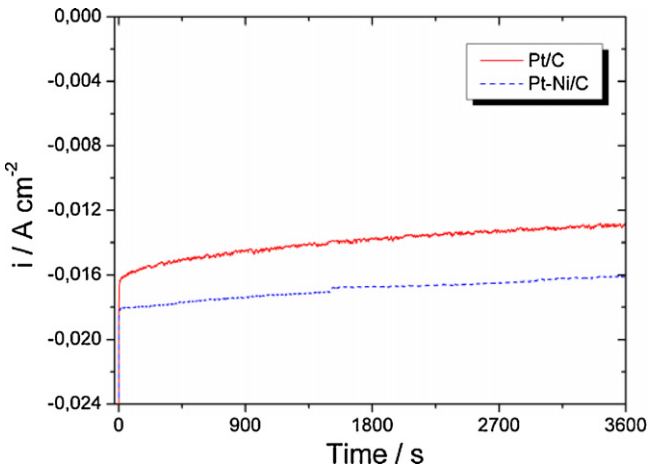

Fig. 5. Chronoamperometry test for oxygen reduction at room temperature on Pt/C and Pt–Ni/C electrocatalysts.

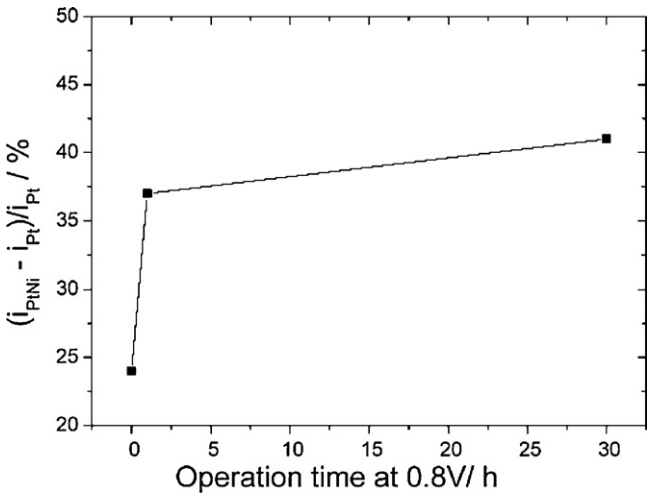

Fig. 7. Difference in the steady state current density of Pt–Ni/C and Pt/C vs. constant potential time.

3.2.2. *Extended constant potential (CP) experiments*

Chronoamperometry measurements carried out on the catalysts after 30 h of constant potential operation at 0.8 V vs. *RHE* indicated that for the Pt–Ni/C the steady state is attained after longer time than for Pt/C. Fig. 6 shows CA curves for 14,000 s of Pt/C and Pt–Ni/C after 30 h of constant potential test. Compared with the as-prepared catalysts, the steady state current density at 0.8 V from CA decreased by 17% for Pt/C and 6% for Pt–Ni/C: as a result, the difference between the steady state current of Pt–Ni/C and Pt/C increases, particularly after the first hour of CP test, as shown in Fig. 7, where the difference in the steady state current density of Pt–Ni/C and Pt/C is plotted against constant potential operation time. The increase of the particle size of Pt/C and Pt–Ni/C catalysts following 30 h of CP at 0.8 V results in a decrease of the active surface area of these catalysts with respect to as-prepared materials. This decreases the activity for the ORR of these catalysts, as observed in the case of Pt/C. On the other hand, the presence of a high amount of NiO_x decreases the ORR activity as (1) it hinders the O_2 flux to Pt active sites and (2) being nickel oxide an insulator material, decreases the electrical conductivity of the catalyst layer. On this basis, the dissolution of Ni oxides during 30 h of constant potential operation should enhance the ORR activity of the Pt–Ni/C catalyst, counteracting the negative effect of the particle growth.

The negative effect of NiO_x presence can be inferred comparing the linear sweep voltammetry (LSV) curves before and after 30 h of CA at 0.8 V. The experimental results are shown in Figs. 8 and 9, with the current density expressed in terms of the geometric surface area. Regarding the as-prepared catalysts, as shown in Fig. 8, the onset potential for the ORR for Pt/C, at about 850 mV, was about 30 mV higher than that of the Pt–Ni catalyst, and the overpotential on Pt–Ni/C at a current density of 0.1 A cm^{-2} was about 30 mV higher compared to that on Pt/C, indicating a slightly higher ORR activity of Pt/C. LSV measurements after 30 h CA at 0.8 V (Fig. 9) indicated that, while the ORR onset potential of Pt/C was almost the same as that of the as-prepared sample, the onset potential of Pt–Ni was about 45 mV higher than that of the as-prepared catalyst. Moreover, the overpotential on Pt–Ni/C at a current density of 0.1 A cm^{-2} was about 100 mV lower compared to that on Pt/C, indicating a higher ORR activity of Pt–Ni/C. This improvement in the ORR activity of the Ni-containing catalyst, as reported in Fig. 7, likely could be ascribed to the loss of NiO_x. As can be seen in Fig. 10, the current density at 0.6 V by LSV for Pt–Ni increases with time, particularly in the first hour (30%) and this behaviour follows the NiO_x loss, which occurs in the first part of the test, as shown in Fig. 3. The current density at 0.6 V for Pt/C, instead, is quite constant.

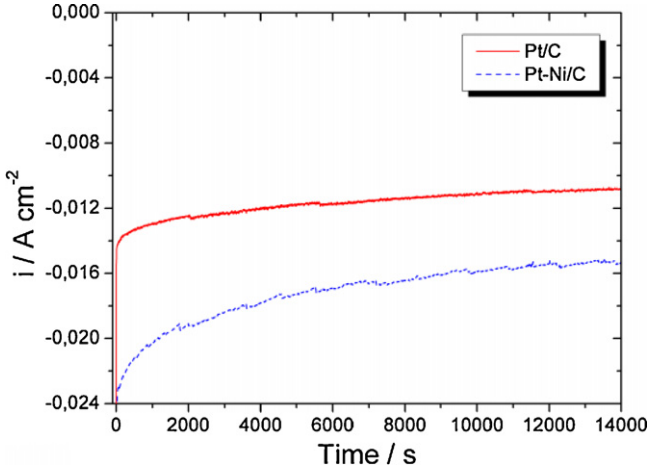

Fig. 6. Chronoamperometry test for oxygen reduction at room temperature on Pt/C and Pt–Ni/C electrocatalysts following 30 h of CP operation at 0.8 V.

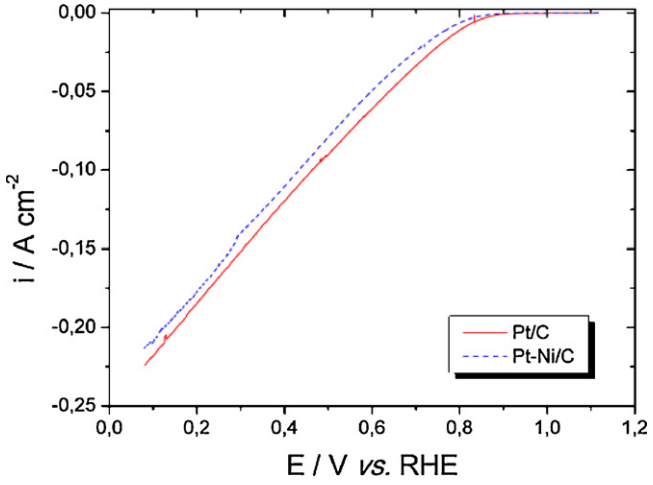

Fig. 8. Linear sweep voltammetry measurements at room temperature in 0.5 M H_2SO_4 on as-prepared Pt–Ni/C and Pt/C electrocatalysts. Current densities normalized with respect to the geometric surface area.

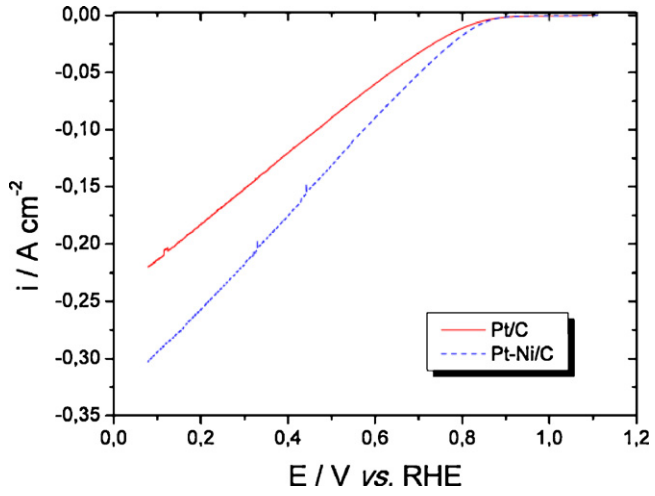

Fig. 9. Linear sweep voltammetry measurements at room temperature in 0.5 M H_2SO_4 on Pt–Ni/C and Pt/C electrocatalysts following 30 h CA at 0.8 V. Current densities normalized with respect to the geometric surface area.

3.2.3. *Catalysts after repetitive potential cycling (RPC)*

As reported by Borup et al. [34], the ageing test by repetitive potential cycling is more severe than under steady-state conditions. As mentioned above, from EDX and XRD measurements it was found that dissolution of not only non-alloyed Ni but also of part of the Pt–Ni alloy takes place. Following the repetitive potential cycling, the Pt–Ni/C catalyst presented an increase of the crystallite size of about 15% with respect to the as-prepared catalysts (see Table 1). The growth of metal particles of supported catalysts by repetitive potential cycling has been reported [35–42]. Also a surface-enrichment with Pt is associated with the potential cycling technique [41]. In most electrochemical works Pt surface enrichment is regarded in terms of dissolution of the less noble component of the alloy. Based on results obtained by EDX and XRD analyses, it can be supposed that the dissolution of Ni and Pt from small-size alloy particles and the re-deposition of Pt on the surface of larger particles occurs. Thus, a Pt layer is formed on the catalyst surface by the dissolution-re-deposition process of Pt (and not of Ni). Fig. 11 shows CA curves of Pt/C and Pt–Ni/C after RPC. By comparing Figs. 5 and 11, it can be concluded that the ORR activity of Pt–Ni/C catalyst following RPC is lower than both as-prepared Pt–Ni/C and cycled Pt/C. The steady state current density at 0.8 V of cycled Pt–Ni/C decreased by 58% with respect to as-prepared

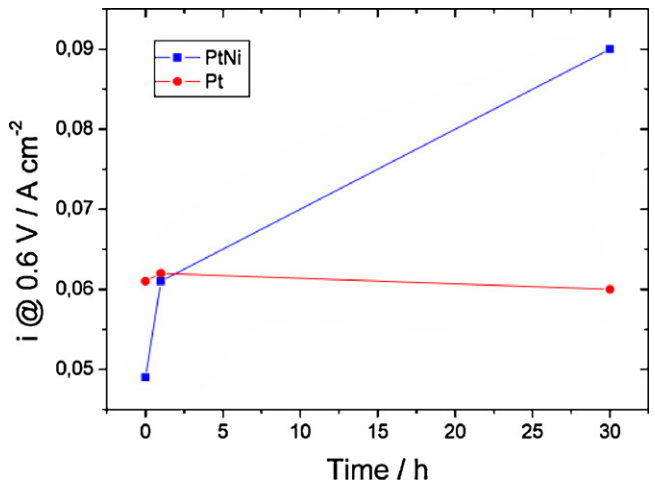

Fig. 10. Current density at 0.6 V by LSV for Pt–Ni/C and Pt/C electrocatalysts vs. constant potential time.

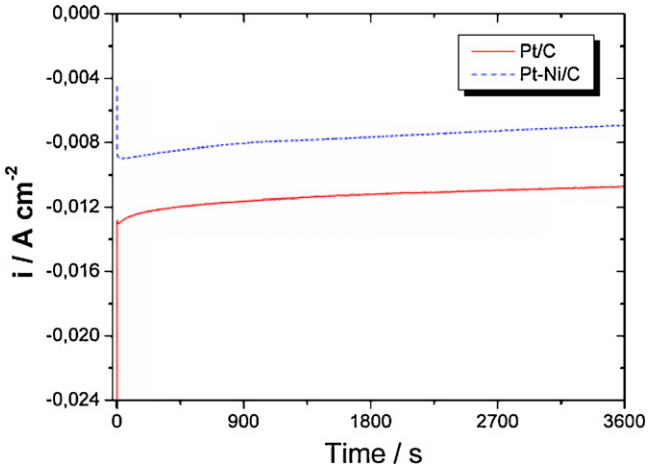

Fig. 11. Chronoamperometry test for oxygen reduction at room temperature on Pt/C and Pt–Ni/C electrocatalysts after repetitive potential cycling.

Pt–Ni/C and 26% with respect to cycled Pt/C. This result depends on the negative effect on the catalytic activity of Pt–Ni/C of both Pt surface enrichment, causing the loss of the positive effect of Ni on the ORR activity, and particle size increase. LSV measurements after RPC showed a slightly higher ORR activity of Pt/C than that of Pt–Ni/C (see Fig. 12), in agreement with the results of CA measurements on samples submitted to RPC. The slightly higher ORR activity of the Pt/C catalyst has to be ascribed to the higher Pt content in the electrode: being total metal amount in the cathode 0.4 mg cm^{-2}, in the case of pure Pt the Pt loading is 0.4 mg cm^{-2}, while in the case of Pt–Ni/C the Pt loading is about 0.29 mg cm^{-2}.

The histogram of the steady-state current density of oxygen reduction from CA of Pt–Ni/C and Pt/C catalysts before and after the stability tests is shown in Fig. 13a, and the histogram of the difference in the steady-state current densities at 0.8 V before (i_o) and after (i_{at}) ageing tests for Pt/C and Pt–Ni/C is shown in Fig. 13b. As can be seen comparing Figs. 9 and 12, in the case of Pt/C the decrease of the steady-state current density of oxygen reduction is independent of the type of stability test, depending only on the increase of particle size. For the Pt–Ni/C, instead, the decrease of the steady-state current density of oxygen reduction depends on the type of durability test. As discussed above, during 30 h of constant potential operation at 0.8 V the loss of NiO_x balances the increase in particle size, while during RPC Pt surface enrichment and

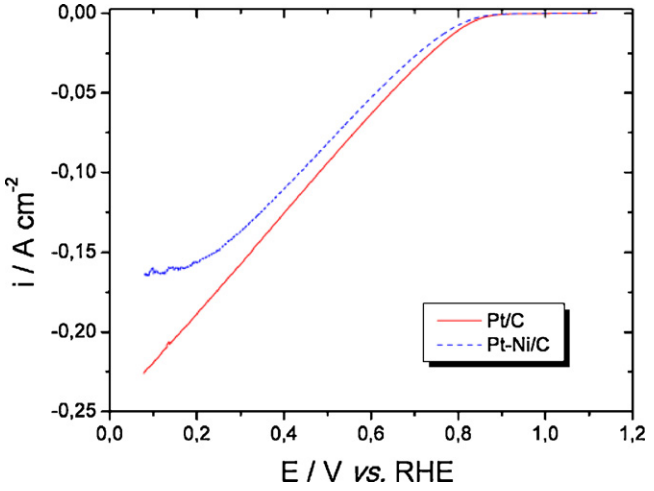

Fig. 12. Linear sweep voltammetry measurements at room temperature in 0.5 M H_2SO_4 on Pt–Ni/C and Pt/C electrocatalysts following repetitive potential cycling. Current densities normalized with respect to the geometric surface area.

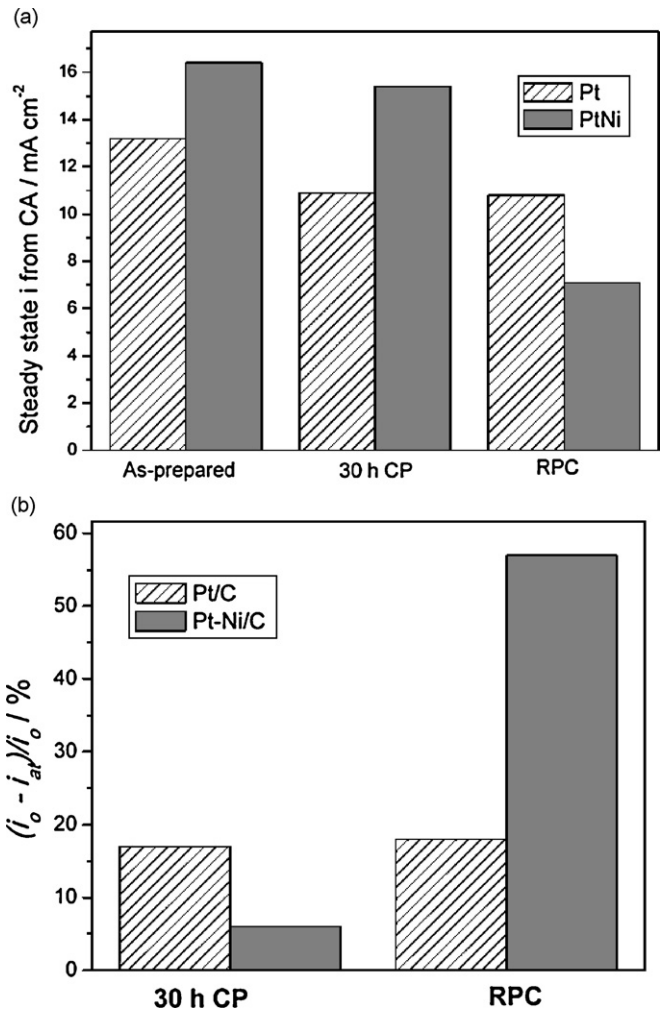

Fig. 13. (a) Histogram of the steady-state current density of oxygen reduction from CA of Pt–Ni/C and Pt/C catalysts before and after stability tests. (b) Histogram of the difference in the steady-state current densities at 0.8 V before (i_o) and after (i_{at}) ageing tests for Pt/C and Pt–Ni/C.

particle size increase cause a more severe negative effect on ORR activity.

Summarizing, the change in the ORR activity of the Pt–Ni/C catalyst following durability tests is due to both the 'physical' modification of the electroactive Pt surface area by particle growth and NiO_x loss, and the chemical modification of the catalyst surface by substitution of the Pt–Ni alloy with Pt. As the ORR activity loss of Pt–Ni/C depends on the durability test, it is not possible establish an order of stability between Pt/C and Pt–Ni/C.

4. Conclusions

Carbon supported Pt and Pt–Ni (1:1) were prepared by reduction of Pt and Ni precursors with $NaBH_4$, and submitted to durability tests. As-prepared Pt–Ni catalyst presented higher ORR activity than Pt. Following 30 h of constant potential operation at 0.8 V loss of all non-alloyed Ni, partial dissolution of the Pt–Ni alloy and an increase of the crystallite size was observed for the Pt–Ni/C catalyst. The ORR activity of the Pt–Ni/C catalyst was almost stable, whereas the ORR activity of Pt/C slightly decreased with respect to the as-prepared catalysts. This result was ascribed to the positive effect of NiO_x loss counteracting the negative effect due to particle size increase. After repetitive potential cycling, instead, the ORR activity of the Pt–Ni/C catalyst was lower than both as-prepared Pt–Ni/C and cycled Pt/C. This result depends on the negative effect of both Pt surface enrichment, causing the loss of the positive effect of alloyed Ni on the ORR activity, and particle size increase. Summarizing, while the ORR activity loss of Pt/C under PEMFC conditions is independent of the ageing test that of Pt–Ni/C strongly depends on the durability experiment. So it is not possible to affirm that Pt–Ni/C is more/less stable than Pt/C without indicating the type of stability test used to make the comparison.

Acknowledgments

The authors thank the Conselho Nacional de Desenvolvimento Científico e Tecnológico (CNPq, Proc. 310151/2008-2) for financial assistance to the project. Thanks are also due to the Brazilian Synchrotron Light Laboratory (LNLS) for helping with the XAS experiments.

References

[1] S. Gottesfeld, T.A. Zawodzinski, Polymer electrolyte fuel cells, in: R.C. Alkire, H. Gerischer, D.M. Kolb, C.W. Tobias (Eds.), Advances in Electrochemical Science and Engineering, vol. 5, 1st ed, Wiley–VCH, Weinheim, 1997, p. 195.
[2] V. Jalan, E.J.J. Taylor, J. Electrochem. Soc. 130 (1983) 2299.
[3] B.C. Beard, P.N. Ross, J. Electrochem. Soc. 133 (1986) 1839.
[4] M.T. Paffett, G.J. Berry, S. Gottesfeld, J. Electrochem. Soc. 135 (1988) 1431.
[5] B.C. Beard, P.N. Ross, J. Electrochem. Soc. 137 (1990) 3368.
[6] S. Mukerjee, S. Srinivasan, J. Electroanal. Chem. 357 (1993) 201.
[7] M. Watanabe, K. Tsurumi, T. Mizukami, T. Nakamura, P. Stonehart, J. Electrochem. Soc. 141 (1994) 2659.
[8] T. Toda, H. Igarashi, H. Uchida, M. Watanabe, J. Electrochem. Soc. 146 (1999) 3750.
[9] M. Min, J. Cho, K. Cho, H. Kim, Electrochim. Acta 45 (2000) 4211.
[10] U.A. Paulus, G.G. Scherer, A. Wokaun, T.J. Schmidt, V. Stamenkovic, V. Radmilovic, N.M. Markovic, P.N. Ross, J. Phys. Chem. B 106 (2002) 4181.
[11] E. Antolini, R.R. Passos, E.A. Ticianelli, Electrochim. Acta 48 (2002) 263.
[12] S. Mukerjee, S. Srinivasan, M.P. Soriaga, J. McBreen, J. Electrochem. Soc. 142 (1995) 1409.
[13] V. Stamenkovic, T.J. Schmidt, P.N. Ross, N.M. Markovic, J. Phys. Chem. B 106 (2002) 11970.
[14] V. Stamenkovic, T.J. Schmidt, P.N. Ross, N.M. Markovic, J. Electroanal. Chem. 554–555 (2003) 191.
[15] J.-F. Drillet, A. Ee, J. Friedemann, R. Kotz, B. Schnyder, V.M. Schmidt, Electrochim. Acta 47 (2002) 1983.
[16] N. Wakabayashi, M. Takeichi, H. Uchida, M. Watanabe, J. Phys. Chem. B 109 (2005) 5836.
[17] H. Yang, W. Vogel, C. Lamy, N. Alonso-Vante, J. Phys. Chem. B 108 (2004) 11024.
[18] E. Antolini, J.R.C. Salgado, E.R. Gonzalez, J. Power Sources 160 (2006) 957.
[19] H.R. Colon-Mercado, H. Kim, B.N. Popov, Electrochem. Commun. 6 (2004) 795.
[20] S.C. Zignani, E. Antolini, E.R. Gonzalez, J. Power Sources 182 (2008) 83.
[21] E. Antolini, Mater. Chem. Phys. 78 (2003) 563.
[22] J. McBreen, W.E. O'Grady, K.I. Pandya, R.W. Roffman, D.E. Sayers, Langmuir 3 (1987) 428.
[23] H. Tolentino, J.C. Cezar, D.Z. Cruz, V. Compagnon-Caillol, E. Tamura, M.C. Alves, J. Synchrotron Radiat. 5 (1998) 521.
[24] T. Ressler, J. Phys. IV C2 (7) (1997) 269.
[25] K.I. Pandya, R.W. Roffman, J. McBreen, W.E. O'Grady, J. Electrochem. Soc. 137 (1990) 383.
[26] J.B.A.C. van Zon, D.C. Konigsberger, H.F.J. Van't Blik, D.E. Sayers, J. Chem. Phys. 82 (1985) 5742.
[27] E. Antolini, J.R.C. Salgado, E.R. Gonzalez, Appl. Catal. B 63 (2006) 137.
[28] K. Endo, K. Nakamura, Y. Katayama, T. Miura, Electrochim. Acta 49 (2004) 2503.
[29] E. Antolini, J.R.C. Salgado, A.M. dos Santos, E.R. Gonzalez, Electrochem. Solid State Lett. 8 (2005) A226.
[30] E. Antolini, J.R.C. Salgado, E.R. Gonzalez, J. Power Sources 155 (2006) 161.
[31] S. Mukerjee, S. Srinivasan, M.P. Soriaga, J. McBreen, J. Phys. Chem. 99 (1995) 4577.
[32] S. Mukerjee, J. McBreen, J. Electroanal. Chem. 448 (1998) 163.
[33] E. Antolini, J.R.C. Salgado, M.J. Giz, E.R. Gonzalez, Int. J. Hydrogen Energy 30 (2005) 1213.
[34] R.L. Borup, J.R. Davey, F.H. Garzon, D.L. Wood, M.A. Inbody, J. Power Sources 163 (2006) 76.
[35] K.S. Han, Y.S. Moon, O.H. Han, K.J. Hwang, I. Kim, H. Kim, Electrochem. Commun. 9 (2007) 317.
[36] W.E. Triaca, A.J. Arvia, J. Appl. Electrochem. 20 (1990) 347.
[37] L.D. Burke, J.J. Borodzinski, K.J. O'Dwyer, Electrochim. Acta 36 (1990) 967.
[38] L.D. Burke, K.J. O'Dwyer, Electrochim. Acta 37 (1991) 43.
[39] L.D. Burke, M.B.C. Roche, J. Electroanal. Chem. 137 (1982) 175.
[40] K. Kinoshita, J.T. Lundquist, P. Stonehart, J. Electroanal. Chem. Interfacial Electrochem. 48 (1973) 157.
[41] L.D. Burke, E.J.M. O'Sullivan, J. Electroanal. Chem. 112 (1980) 247.
[42] C.C. Hu, K. Liu, Electrochim. Acta 44 (1999) 2727.